Published in final edited form as:
Biomacromolecules. 2012 November 12; 13(11): 3723–3729. doi:10.1021/bm301197h.

Salt-leached silk scaffolds with tunable mechanical properties

Danyu Yao[a], **Sen Dong**[b], **Qiang Lu**[a,*], **Xiao Hu**[c,d], **David L Kaplan**[c], **Bingbo Zhang**[e], and **Hesun Zhu**[f]

[a]National Engineering Laboratory for Modern Silk, College of Textile and Clothing Engineering, Soochow University, Suzhou 215123, People's Republic of China

[b]Huludao City Central Hospital, Huludao 125000, People's Republic of China

[c]Department of Biomedical Engineering, Tufts University, Medford, MA 02155, USA

[d]Department of Physical and Astronomy, Rowan University, Glassboro, NJ 08028, USA

[e]The institute for Advanced Materials and Nano Biomedicine, School of Medicine, Tongji University, Shanghai 200092, People's Republic of China

[f]Research Center of Materials Science, Beijing Institute of Technology, Beijing, 100081, People's Republic of China

Abstract

Substrate mechanical properties have remarkable influences on cell behavior and tissue regeneration. Although salt-leached silk scaffolds have been used in tissue engineering, applications in softer tissue regeneration can be encumbered with excessive stiffness. In the present study, silk-bound water interactions were regulated by controlling processing to allow the preparation of salt-leached porous scaffolds with tunable mechanical properties. Increasing silk-bound water interactions resulted in reduced silk II (beta-sheet crystal) formation during salt-leaching, which resulted in a modulus decrease in the scaffolds. The microstructures as well as degradation behavior were also changed, implying that this water control and salt-leaching approach can be used to achieve tunable mechanical properties. Considering the utility of silk in various fields of biomedicine, the results point to a new approach to generate silk scaffolds with controllable properties to better mimic soft tissues, by combining scaffold preparation methods and silk self-assembly in aqueous solutions.

Keywords

Silk; Biomaterials; Mechanical properties; Scaffolds

1. Introduction

Matrix stiffness is increasingly appreciated as an important mediator of cell behavior to regulate cell signaling, with effects on growth, survival, and motility.[1] Mesenchymal stem cells (MSCs) specify lineage and commit to phenotype with sensitivity to tissue-level stiffness.[2] When cultured in matrices with different stiffness, such as brain, muscle and bone, MSCs differentiated into neurogenic, myogenic, and osteogenic cells, respectively.[2] Besides stem cells, tissue-specific cells including fibroblasts, myocytes, neurons, and others also sense matrix stiffness to regulate the formation and maintenance of tissues.[3, 4] These

Corresponding author: Qiang Lu, Tel: (+86)-512-67061649; Lvqiang78@suda.edu.cn.

studies indicate that scaffolds used in different tissue regeneration needs should mimic the rigidity of the target tissues to improve biological outcomes.[4–6]

In recent years, silk fibroin has been explored for different biomedical applications due to its biocompatibility, biodegradability, and mechanical properties.[7–11] Silks in biomaterial scaffolds provide support matrices for cells, including fibroblasts, osteoblasts, hepatocytes, and stem cells, as well as scaffolding for tissue engineering bone, ligaments, cartilage, blood vessels, skin, and nerves, among others.[12–16] Although a number of methods have been used to prepare silk-based scaffolds,[17–22] the salt-leaching method is widely used due to effectiveness, efficiency and ease of process. However, salt-leached silk scaffolds generally are stiff because of silk II (beta-sheet crystal) formation, leaving a gap in utility for some soft tissues.[17, 23] Until now, there is no effective way to control rigidity of the salt-leached silk scaffolds. Thus, for such needs, silk hydrogels have generally been utilized. However, hydrogels are less stable to cell and tissue culture. Therefore, options to match the stiffness of very soft tissues with a porous mechanically stable silk salt-leached matrix would provide additional options for the study of soft tissue regeneration using silk biomaterials.

In our recent studies it was found that silk-bound water interactions partly restrained silk II formation.[24, 25] When silk-bound water interactions were enhanced, more of the silk maintained random coil structure after thermal treatment, implying the possibility that improving silk-bound water interactions might be effective at controlling silk crystal composition, and thus softer mechanical properties.

The goal of the present study was to utilize control of the interactions between silk and water to prepare silk porous scaffolds with tunable mechanical properties through salt-leaching, in order to generate softer silk substrates. Nanostructure features as well as degradation behavior were investigated to confirm that the combination of salt-leaching and silk pretreatment was an effective approach to tune the scaffolds to generate systems closer in mechanics to softer natural tissues.

2. Materials and methods

2.1 Preparation of silk solutions

Bombyx mori fibroin solutions were prepared according to our previously published procedures[26] Cocoons were boiled for 30 min in an aqueous solution of 0.02 M Na_2CO_3 and then rinsed thoroughly with distilled water to extract the sericin proteins. The process was repeated three times to ensure that sericin proteins were completely extracted. After drying the extracted silk fibroin was dissolved in 9.3 M LiBr solution at 60°C for 4h, yielding a 20% (w/v) solution. This solution was dialyzed against distilled water using Slide-a-Lyzer dialysis cassettes (Pierce, molecular weight cut-off 3,500) for 72h to remove the salt. The solution was centrifuged at 9000 r/min for 20 min and 4 °C, repeat three times, to remove silk aggregates formed during the process. The final concentration of aqueous silk solution was about 5 wt%, determined by weighing the remaining solid after drying.

2.2 Preparation of silk scaffolds

The drying rate of the solution was controlled with lids with different air exchange rates at 60°C. Then fresh silk solution was concentrated to 25 wt% after 2 days and 5 days, respectively. After these concentrated solutions were diluted to 5 wt% with distilled water, salt-leached silk scaffolds were prepared from the solutions according to our previously reported procedures.[17, 23] 4 g of granular NaCl (particle size 350–450μm) was added slowly to a cylindrically-shaped container with 2 ml silk solution. As controls, salt-leached silk scaffolds were also prepared from freshly prepared silk solution using the same procedure.

The scaffolds prepared from the slow-concentrated solution (5 days), fast-concentrated solution (2 days) and fresh solution are termed SC-S, FC-S and F-S, respectively.

2.3 Differential scanning calorimetry (DSC)

For DSC experiments, all silk solutions were flash frozen and dried in liquid nitrogen to preserve original structures as accurately as possible based on our previous studies.[24, 27]. The thermal properties of the samples were measured in a TA instrument Q100 DSC (TA Instruments, New Castle, DE) under a dry nitrogen gas flow of 50 ml min^{-1}. Temperature-modulated differential scanning calorimetry (TMDSC) measurements were performed using a TA instrument Q100 equipped with a refrigerated cooling system. The samples were heated at 2°C min^{-1} with a modulation period of 60s and a temperature amplitude of 0.318°C.

2.4 Fourier transform infrared (FTIR)

The structure of the various scaffolds was analyzed by FTIR on a NICOLET FTIR 5700 spectrometer (Thermo Scientific, FL, America). Slices with thickness of about 1 mm were cut from the scaffolds with a razor blade in liquid nitrogen. For each measurement, 64 scans were coded with a resolution of 4 cm^{-1}, with the wavenumber ranging from 400 to 4,000 cm^{-1}.

2.5 X-ray diffraction (XRD)

Crystal structure was determined by X-ray diffraction (XRD). The experiments were conducted with an X-ray diffractometer (X'Pert-Pro MPD, PANalytical, Almelo, Holland) with CuKa radiation at 40 kV and 30 mA and scanning rate of 0.6min^{-1}.

2.6 Atomic force microscopy (AFM)

For AFM experiments, silk solutions were diluted to below 0.1 wt% to avoid masking the original morphology by multilayers of silk.[24] Two microliters of the diluted SF solution was dropped onto freshly cleaved 4×4 mm^2 mica surfaces. The morphology of silk fibroin in water was observed by AFM (Nanoscope V, Veeco, Plainview, NY, America) in air. A 225 Gm long silicon cantilever with a spring constant of 3 Nm^{-1} was used in tapping mode at 0.5^{-1} Hz scan rate.

2.7 Scanning electron microscopy (SEM)

Cross-sections were prepared by cutting the dried scaffolds with a razor blade in liquid nitrogen. The cross-sections were coated with platinum and examined morphologically by SEM (S-4800, Hitachi, Tokyo, Japan).

2.8 Mechanical properties

The compression properties of specimens (d=15 mm, h=9 mm) were measured with a cross head speed of 2 mm min^{-1} at 25°C using an Instron 3366 testing frame (Instron, Norwood, MA) with a 10N capacity load cell. The mechanical properties of the scaffolds were determined in both dry and wet conditions. For the wet condition the scaffolds were first hydrated in water for 2 h and then measured at 25°C with a cross head speed of 2 mm min^{-1} while the dry samples were measured at 25°C and 65% RH. All samples were measured in triplicates.

2.9 Silk dissolution

The different salt-leached scaffolds were incubated at 37°C in phosphate saline (PBS (40 ml)). Each solution contained an approximately equivalent mass (40±5 mg) of salt-leached

scaffold. Solutions were replenished with fresh PBS daily. At designated time points (1 day, 2 days, 7 days, 14 days and 24 days) the samples were rinsed with distilled water and prepared for mass balance assessment. To know if the scaffolds were stable enough for short term cell culture, a short time dissolution was also executed. Scaffolds were rinsed and prepared for mass balance assessment at designated time points(0.5 h, 1 h, 2 h, 4 h, 8 h, 16 h, 24 h, 32 h, 40 h, 48 h), too.

3. Results and discussion

3.1 Silk solution properties

Silk-bound water interactions restrained the transition from random structures to silk II crystals in our prior studies.[24] Therefore, it was pursued to control silk II formation in the salt-leaching process by adjusting silk-bound water interactions in solution. In our previous studies, it was found that silk fibroin could self-assemble to form different nanostructures following the changes of silk-water interaction [24]. When silk fibroin solution was concentrated slowly, stronger silk fibroin-bound water interaction achieved, which could restrain the silk II formation in the salt-leached process and then result in the changes of the scaffold mechanical properties. In the present study, silk-bound water interactions were enhanced by slow concentrating process according to our previous study.[24] The silk-bound water interactions were characterized by temperature-modulated DSC according to our previous study. Reversing DSC is an effective method to study the interaction between silk fibroin and bound water [24, 28, 29]. As shown in Figure 1, little silk-bound water interactions were found from flash freeze-dried fresh silk solutions. When silk solutions were treated by a fast-concentration process (e.g., water was removed rapidly) (FC-S), the Tg appeared at 49°C, indicating the formation of weak silk-bound water interactions. The Tg of freeze-dried SC-S samples shifted to 62°C, implying stronger silk-bound water interactions formed when the silk solution was treated by the slow-concentrating process. Besides the improvement of silk-bound water interactions, nanostructures of silk in solution also changed in the concentration process. Silk gradually assembled into nano-particles with sizes of several hundred nanometers (Figure 2), which would further affect the final microstructure of salt-leached scaffolds.

3.2 Structural characteristics of salt-leached scaffolds

Silk scaffolds were prepared with the same salt-leaching process but using the solutions with different levels of silk-bound water interactions. The structural changes of these silk scaffolds were determined by FTIR and XRD (Figure 3). The infrared (IR) spectral region within 1700-1500 cm^{-1} is assigned to absorption by the peptide backbones of amide I (1700-1600 cm^{-1}) and amide II (1600-1500 cm^{-1}), which have been commonly used for the analysis of different secondary structures of silk fibroin. The peaks at 1610-1630 cm^{-1} (amide I) and 1510-1520 cm^{-1} (amide II) are characteristic of silk II secondary structure while the peaks at 1630-1650 cm^{-1} and 1520-1540 cm^{-1} are indicative of random coil structures.[30, 31] The amide I and II bands for F-S and FC-S showed strong peaks at 1623 cm^{-1} and 1519cm^{-1}, corresponding to silk II. When the scaffolds were prepared from slow-concentrated silk solutions, besides the absorptions at 1623 cm^{-1} and 1519 cm^{-1}, new bands at 1634 cm^{-1} and 1534 cm^{-1} appeared, indicating more random structures were maintained for SC-S. Deconvolution of these spectta demonstrated a statistically significant decrease in silk II content ($p < 0.05$) from 49.0% to 45.0% and 41.6% for F-S, FC-S and SC-S, respectively. To know whether the structure is stable enough, all the salt-leached scaffolds were also treated by water annealing and methanol annealing processes and then detected by FTIR and XRD. No obvious structural changes were observed for all the scaffolds after water or methanol annealing treatments, indicating the structure stability of the scaffolds (data not showed). The results confirmed the assumption that the transition from random

structure to silk II crystal in salt-leaching process could be regulated by changing silk-bound water interactions.

Structural changes in the silk scaffolds after the different processes were confirmed by XRD (Figure 3B). The strength of the silk II peaks in the XRD curves also decreased for FC-S and SC-S, confirming that the silk-bound water interaction restrained the growth of silk II structure.

3.3 Mechanical properties of salt-leached scaffolds

Matrix stiffness influences cell and tissue features.[4] Salt-leached silk scaffolds generally have a relatively high silk II content, which results in stiffness of scaffolds.[17, 23, 32, 33] Our recent study showed that the transition of silk chains from random coil to silk II could be restrained by control of silk-bound water interactions.[24] By changing silk-bound water interactions in aqueous solution, silk scaffolds with different silk II contents were prepared through the same salt-leaching process, implying the possibility to achieve salt-leached silk scaffolds with tunable mechanical properties. As shown in Figure 5, the modulus of compressibility decreased following this approach. The results confirmed our hypothesis that salt-leached scaffolds with tunable mechanical properties could be achieved through regulating silk-bound water interactions in aqueous solution. Engler et al. had examined the influence of matrix elasticity on the differentiation of human mesenchymal stem cells. [4] Soft matrices with elastic modulus in the range typical of ~ E_{brain} (0.1–1kPa) favored differentiation of mesenchymal stem cells into neuronal-like cells. [4] SC-S had a modulus that is close to that of brain while the stiffness of F-S was similar to that of muscle. The mechanical differences between the scaffolds might be useful to regulate the regeneration of different tissues, which would be confirmed by cell culture in the near future. Although cell cultures are necessary to elucidate the influence of these silk tunable mechanical properties on cell behavior, considering the sensitivity of cells to matrix stiffness,[2–4] the present study has provided an effective way to improve the potential utility of salt-leached silk scaffolds for an even broader range of tissue regeneration options.

3.4 Morphology of salt-leached scaffolds

Following the improved silk-bound water interactions in solution, the silk assembled into nanoparticles with different sizes (Figure 2). The formation of nanoparticles did not impact porous structure formation during salt-leaching. As shown in Figure 6, all the salt-leached scaffolds had highly interconnected porous structures with similar pore sizes (F-S: 386±42μm, FC-S: 388±52μm, SC-S: 383±52μm). However, morphological changes of the macropore walls were observed in the different scaffolds (Figure 7). Rougher morphologies appeared with the scaffolds derived from silk solutions containing more of these particles. Following the increase of silk particles in solution, more particles with size ranges from 400 nm to 4μm aggregated on the surface of the macropore walls. The particles also had rough surfaces (Figure 7d), which might promote cell adhesion in vitro or in vivo.

3.5 Dissolution

To functionally assess the differences in the scaffolds, the dissolution of the scaffolds was assessed (Figure 8). The salt-leached scaffolds dissolved slowly in PBS solution, losing 34%, 48% and 70% mass after 2 weeks, and then 72%, 85% and 88% mass after 24 days when the scaffolds were prepared from fresh solution (F-S), fast concentrated solution (FC-S) and slowly concentrated solution (SC-S), respectively. Statistical calculation indicated that the degradation rates of F-S, FC-S and SC-S samples had significant difference at 7 and 14 days while only F-S and SC-S had significant different degradation rate at 24 days. The results indicated that dissolution behavior of the salt-leached silk scaffolds could be regulated by changing the silk-bound water interactions in solution. The initial dissolution

behaviors of different silk scaffolds were also studied (Figure 9). A few of unstable silk structures dissolved within 4 hours, without significant morphological changes for all the scaffolds (Figure 9)

4. Conclusions

Salt-leached silk scaffolds with tunable mechanical properties were prepared by changing silk-bound water interactions in solution. Enhancing silk-bound water interactions in silk solutions allowed the transition from random coil structures to silk II in the salt-leaching process was partly restrained, resulting in decreased scaffold stiffness. Thus the preparation of silk salt-leached scaffolds with more controllable or tunable properties was feasible. Present findings provide an effective method to prepare silk-based scaffolds with tunable properties and should not be limited to salt leached scaffolds. We anticipate that this approach of pre-organizing the silk solution features will impact other modes of silk materials fabrication as well.

Acknowledgments

We thank the Priority Academic Program Development of Jiangsu Higher Education Institutions (PAPD) and National Natural Science Foundation of China (21174097) for support of this work. We also thank the National Institues of Health (NIH) P41 Resource Center on Tissue Engineering, Ph.D. Programs Foundation of Ministry of Education of China (201032011200009), the Key Natural Science Foundation of the Jiangsu Higher Education Institutions of China (11KGA430002) as well as the Opening Project of National Engineering Laboratory for Modern Silk, Soochow University for support of this work.

References

1. Wells RG. Hepatology. 2008; 47:1394–1400. [PubMed: 18307210]
2. Engler AJ, Sen S, Sweeney HL, Discher DE. Cell. 2006; 126:677–689. [PubMed: 16923388]
3. Saez A, Ghibaudo M, Buguin A, Silberzan P, Ladoux B. PNAS. 2007; 104:8281–8286. [PubMed: 17488828]
4. Discher DE, Janmey P, Wang YL. Science. 2005; 310:1139–1143. [PubMed: 16293750]
5. Jones JR, Ehrenfried LM, Hench LL. Biomaterials. 2006; 27:964–973. [PubMed: 16102812]
6. Badylak SF, Freytes DO, Gilbert TW. Acta Biomater. 2009; 5:1–13. [PubMed: 18938117]
7. Jin HJ, Park J, Valluzi R, Cebe P, Kaplan DL. Biomacromolecules. 2004; 5:711–717. [PubMed: 15132651]
8. Jiang CY, Wang XY, Gunawidjaja R, Lin YH, Gupta MK, Kaplan DL, Naik RR, Tsukruk VV. Adv Funct Mater. 2007; 17:2229–2237.
9. Liu HF, Fan HB, Wang Y, Toh SL, Goh JCH. Biomaterials. 2008; 29:662–674. [PubMed: 17997479]
10. Vepari C, Kaplan DL. Prog Polym Sci. 2007; 32:991–1007. [PubMed: 19543442]
11. Wang XQ, Wenk E, Matsumoto A, Meinel L, Li CM, Kaplan DL. J Control Release. 2007; 117:360–370. [PubMed: 17218036]
12. Altman GH, Diaz F, Jakuba C, Calabro T, Horan RL, Chen JS, Lu H, Richmond J, Kaplan DL. Biomaterials. 2003; 24:401–416. [PubMed: 12423595]
13. Marolt D, Augst A, Freed LE, Vepari C, Fajardo R, Patel N, Gray M, Farley M, Kaplan DL, Vunjak-Novakovic G. Biomaterials. 2006; 27:6138–6149. [PubMed: 16895736]
14. Zhang YF, Fan W, Ma ZC, Wu CT, Fang W, Liu G, Xiao Y. Acta Biomater. 2010; 6:3021–3028. [PubMed: 20188872]
15. Wang Y, Bella E, Lee CSD, Migliaresi C, Pelcastre L, Schwartz Z, Boyan BD, Motta A. Biomaterials. 2010; 31:4672–4681. [PubMed: 20303584]
16. Huang S, Fu XB. J Control Release. 2010; 142:149–159. [PubMed: 19850093]
17. Nazarov R, Jin HJ, Kaplan DL. Biomacromolecules. 2004; 5:718–726. [PubMed: 15132652]
18. Lv Q, Feng QL. J Mater Sci Mater M. 2006; 17:1349–1356. [PubMed: 17143767]

19. Tamada Y. Biomacromolecules. 2005; 6:3100–3106. [PubMed: 16283733]
20. Zhang XH, Baughman CB, Kaplan DL. Biomaterials. 2008; 29:2217–2227. [PubMed: 18279952]
21. Lu Q, Zhang X, Hu X, Kaplan DL. Macromol Biosci. 2010; 10:289–298. [PubMed: 19924684]
22. Rockwood DN, Preda RC, Yucel T, Wang X, Lovett ML, Kaplan DL. Nature Protocols. 2011; 6:1612–1631.
23. Kim UJ, Park J, Kim HJ, Wada M, Kaplan DL. Biomaterials. 2005; 26:2775–2785. [PubMed: 15585282]
24. Lu Q, Zhu HS, Zhang CC, Zhang F, Zhang B, Kaplan DL. Biomacromolecules. 2012; 13:826–832. [PubMed: 22320432]
25. Lu Q, Hu X, Wang XQ, Kluge JA, Lu SZ, Cebe P, Kaplan DL. Acta Biomater. 2010; 6:1380–1387. [PubMed: 19874919]
26. Lu Q, Wang XL, Lu SZ, Li MZ, Kaplan DL, Zhu HS. Biomaterials. 2011; 32:1059–1067. [PubMed: 20970185]
27. Leisk GG, Lo TJ, Yucel T, Lu Q, Kaplan DL. Adv Mater. 2010; 22:710–715.
28. Hu X, Kaplan DL, Cebe P. Macromolecules. 2006; 39:6161–6170.
29. Hu X, Kaplan DL, Cebe P. Macromolecules. 2008; 41:3939–3948.
30. Jin HJ, Park J, Karageorgiou V, Kim UJ, Valluzzi R, Cebe P, Kaplan DL. Adv Funct Mater. 2005; 15:1241–1247.
31. Simmons H, Michal CA, Jelinski LW. Science. 1996; 271:84–84. [PubMed: 8539605]
32. Zhang XH, Cao CB, Ma XL, Li YA. J Mater Sci Mater Med. 2012; 23:315–324. [PubMed: 22076527]
33. Yan LP, Oliveira JM, Oliveira AL, Caridade SG, Mano JF, Reis RL. Acta Biomater. 2012; 8:289–301. [PubMed: 22019518]

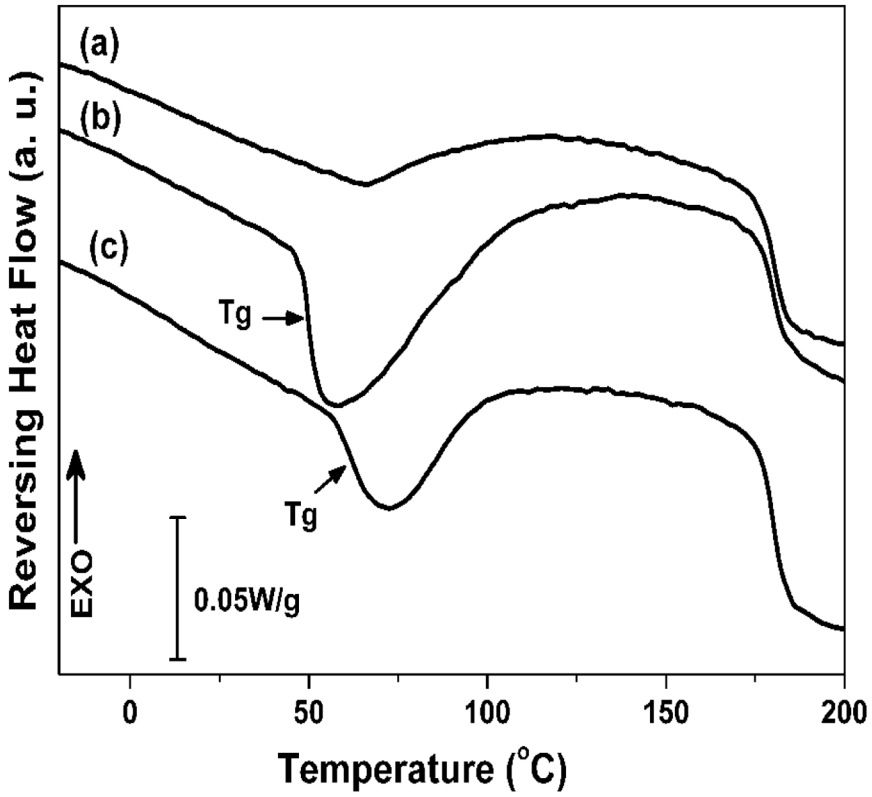

Figure 1.
TMDSC curves for silk solutions with different silk-bound water interactions. The samples are as follows: (a) fresh solution; (b) fast concentrated solution; (c) slow concentrated solution. The treated solutions were diluted to same concentration with fresh solution and then flash freeze-dried in liquid nitrogen to preserve the original structures.

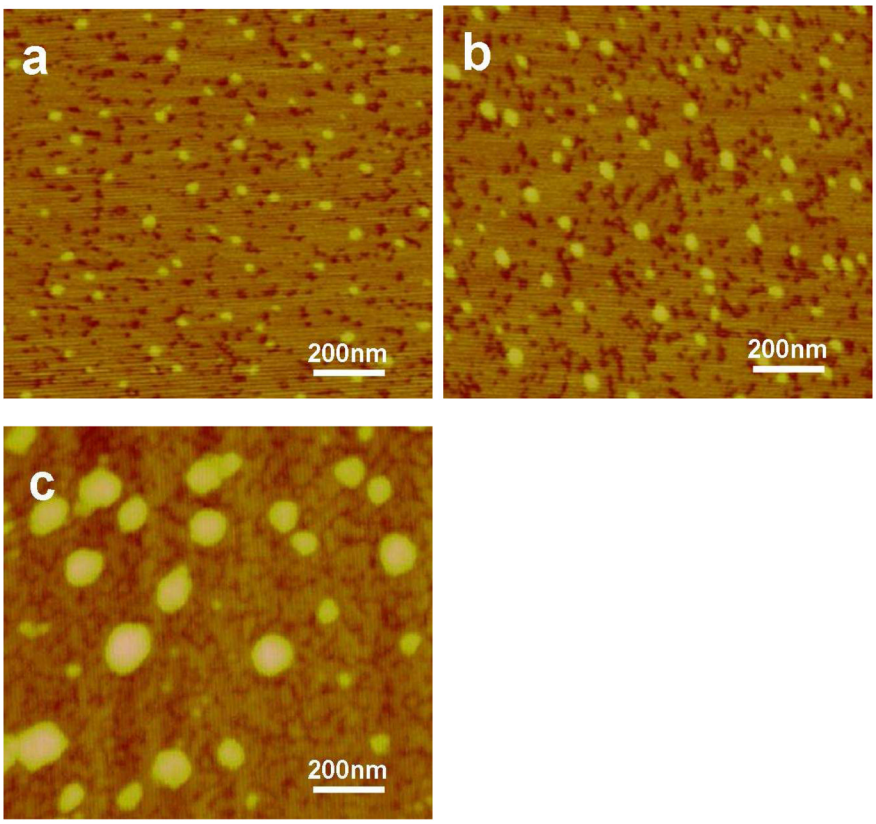

Figure 2.
AFM images of different silk solutions. The samples are as follows: (a) fresh solution scaffold; (b) fast concentrated solution; (c) slow concentrated solution.

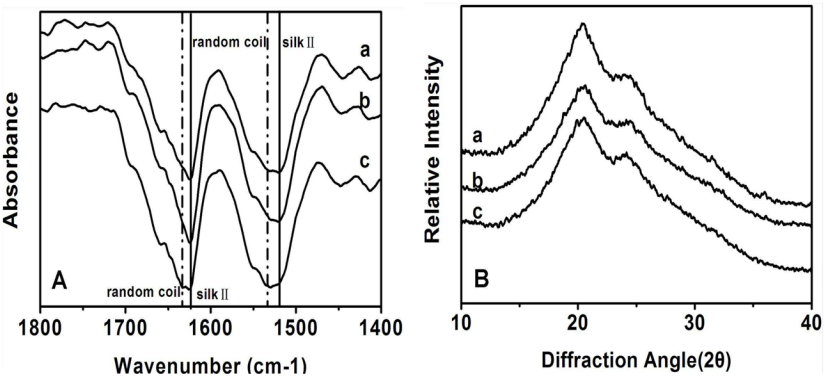

Figure 3.

FTIR (A) and XRD curves (B) for silk scaffolds with different silk-bound water interactions. The samples are as follows: (a) F-S, the scaffolds derived from fresh solution; (b) FC-S, the scaffolds derived from fast concentrated solution; (c) SC-S, the scaffolds derived from slow concentrated solution.

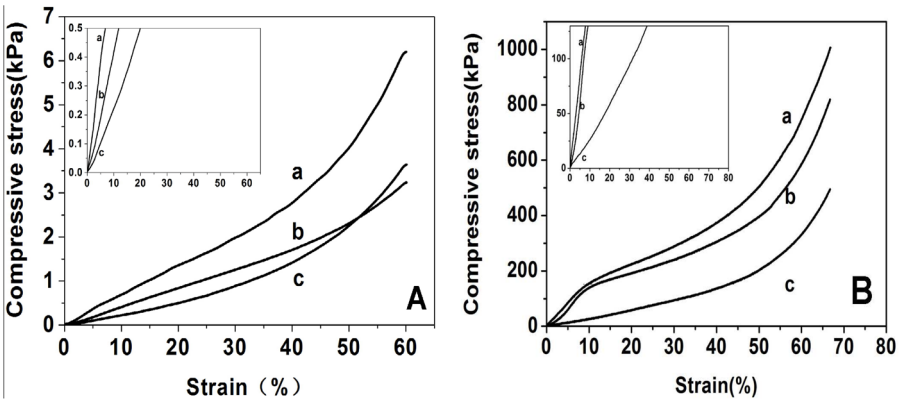

Figure 4.

Typical stress-strain curves of silk scaffolds in wet (A) and dry (B) conditions: (a) F-S, the scaffolds derived from fresh solution; (b) FC-S, the scaffolds derived from fast concentrated solution; (c) SC-S, the scaffolds derived from slow concentrated solution.

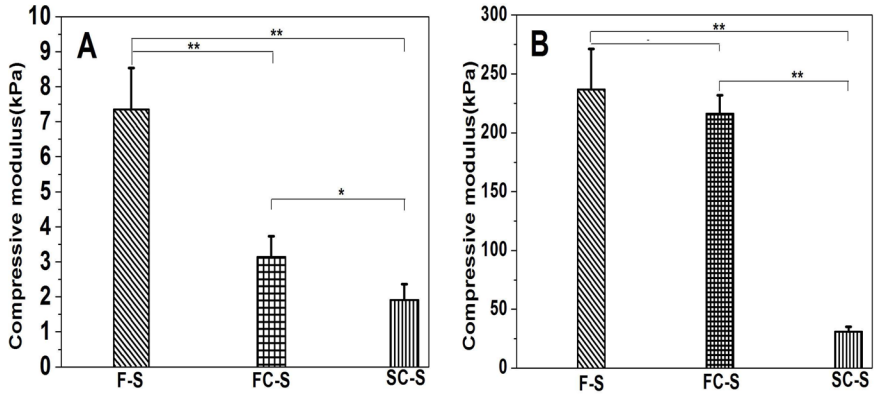

Figure 5.

Compressive modulus of silk scaffolds in wet (A) and dry (B) conditions: the "**"indicates the comparisons are statistically very significant, and the "*"indicates the comparisons are statistically significant. (a) F-S, the scaffolds derived from fresh solution; (b) FC-S, the scaffolds derived from fast concentrated solution; (c) SC-S, the scaffolds derived from slow concentrated solution.

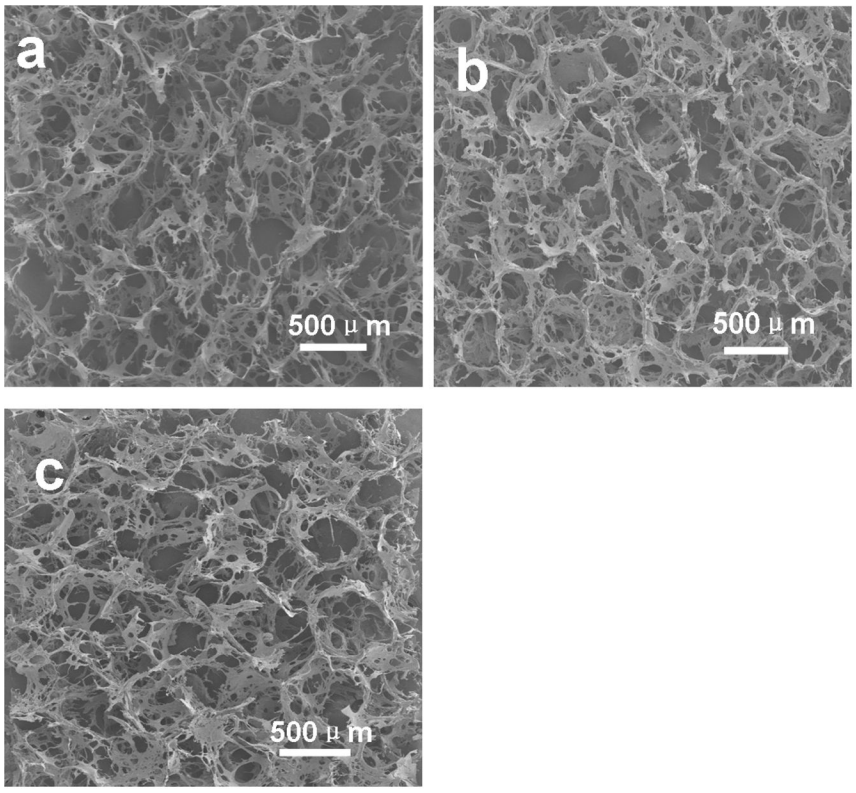

Figure 6.
SEM images of silk scaffolds. (a) F-S, the scaffolds derived from fresh solution; (b) FC-S, the scaffolds derived from fast concentrated solution; (c) SC-S, the scaffolds derived from slow concentrated solution.

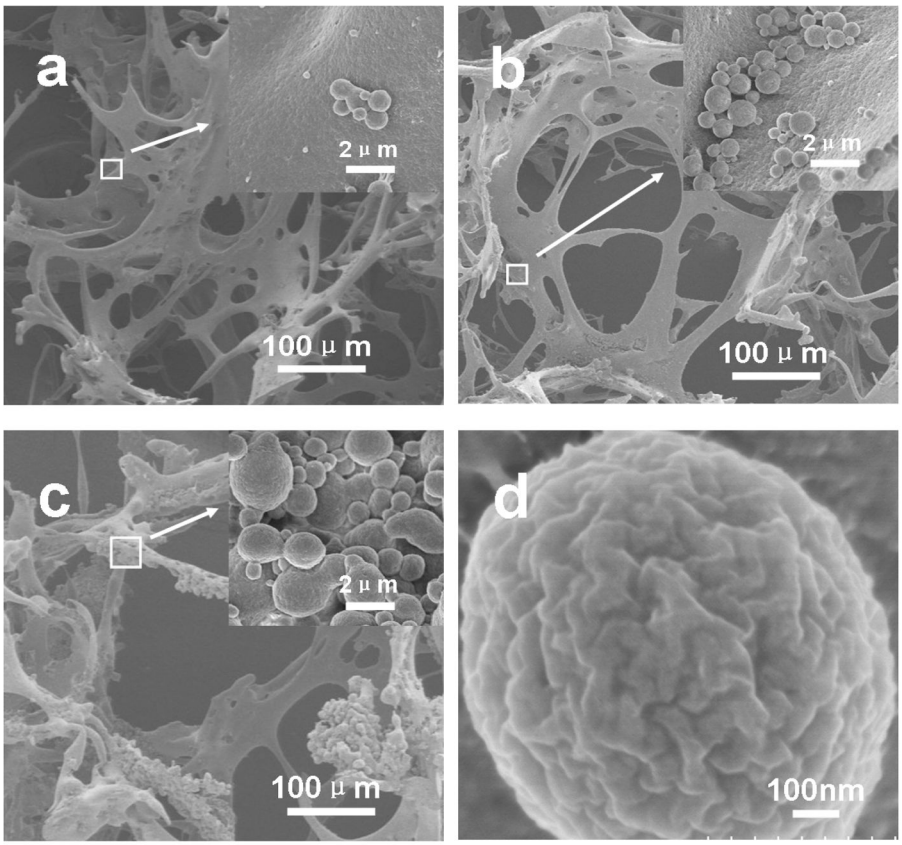

Figure 7.
SEM images of silk scaffolds. (a) F-S, the scaffolds derived from fresh solution; (b) FC-S, the scaffolds derived from fast concentrated solution; (c) SC-S, the scaffolds derived from slow concentrated solution, and (d) the morphology of the spheres in the scaffolds.

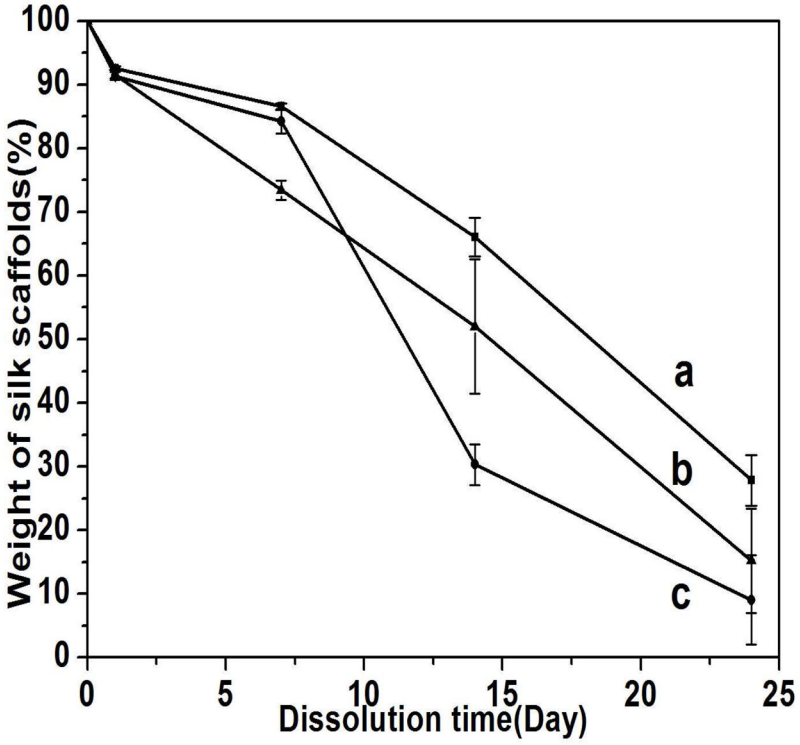

Figure 8.
Dissolution of silk scaffolds in PBS solution within 24 days: (a) F-S, the scaffolds derived from fresh solution, (b) FC-S, the scaffolds derived from fast concentrated solution, (c) SC-S, the scaffolds derived from slow concentrated solution

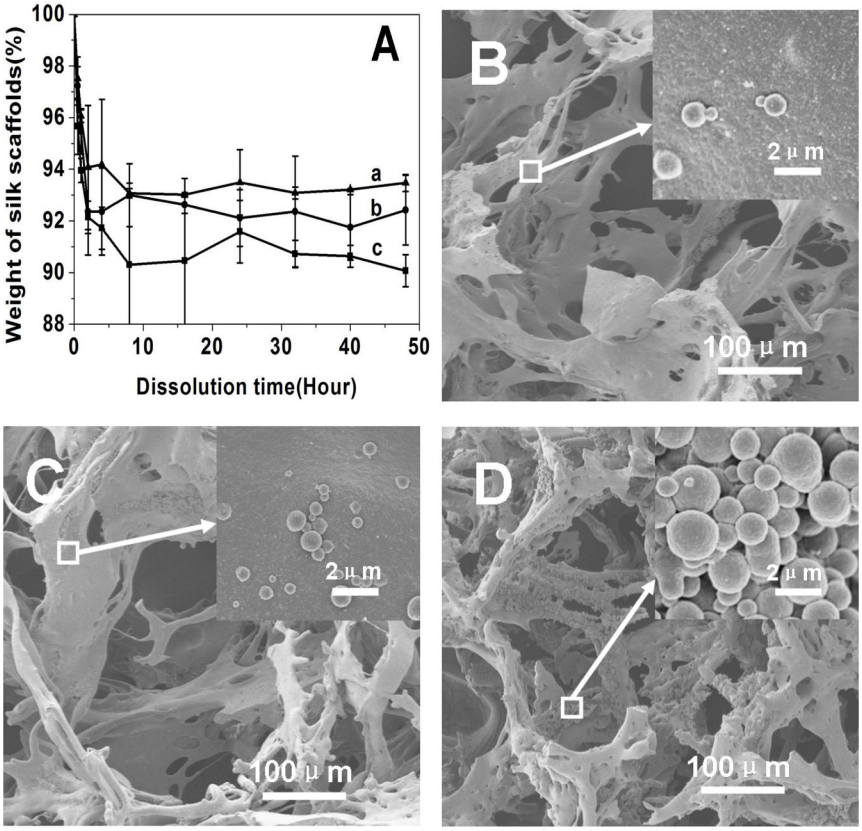

Figure 9.
Dissolution of silk scaffolds in PBS solution within 48 hours (A): (a) F-S, the scaffolds derived from fresh solution, (b) FC-S, the scaffolds derived from fast concentrated solution, (c) SC-S, the scaffolds derived from slow concentrated solution; and the SEM images of silk scaffolds after cultured in PBS for 4 hours: (B) F-S, (C) FC-S, and (D) SC-S.